S. M. Hai[1]

Senior Research Engineer,
Westinghouse Research and Development Center,
Pittsburgh, Pa. Assoc. Mem. ASME

Pressure Development in the Entrance Region and Fully Developed Region of Generalized Channel Turbulent Flows

In this paper, the pressure drops in the developing length of generalized turbulent channel flows are investigated, and the effects of Reynolds number and distance from the channel entrance are examined. The numerical method is also used to predict the pressure drops in simple channel flows for very high Reynolds numbers (of the order of 100,000). Excellent agreement is obtained between experimental data and numerical predictions.

Significant Contribution of This Paper

Generalized turbulent channel flows, i.e., turbulent flows occurring in channels one wall of which is in motion, have important and immediate technical applications in the prediction of bearing performance associated with the hydrodynamic lubrication of a sleeve bearing, and in the design of tube flight vehicles which are under consideration for transportation systems. In addition to these, such flows are sufficiently basic to invite intrinsic interest.

This paper presents the first attempt in the published literature to analyze the pressure development in the entrance region of generalized turbulent channel flows under the influence of both pressure and shear forces. This work is expected to lay the foundation for future research in this field.

Introduction

Generalized turbulent channel flows, i.e., turbulent flows occurring in channels one wall of which is in motion, have important and immediate technical applications. One such application which may come to mind is associated with the hydrodynamic lubrication of a sleeve bearing; here the circumferential shear flow is coupled to both a parallel and an orthogonal pressure flow. Prediction of bearing performance in the turbulent regime is becoming vital to industry due to today's trend toward higher rotational speeds, the use of lower viscosity fluids as lubricants and the ever-increasing size of rotating machinery. The type of flow in bearings varies from pure shear flow to shear flow coupled with pressure flows. Successful design of such bearings will depend upon an understanding of the nature of turbulent flow for the aforementioned flow conditions. In developing a consistent turbulent lubrication theory, in which all significant effects are accounted for, a thorough and basic knowledge of occurring flow, i.e., the generalized turbulent channel flow, is essential. Analytical expressions for the predictions of pressure development, velocity development, etc., must be available for design purposes, so that the overall performance of the bearing may be analyzed.

Another possible future application of the generalized channel flows involves the tube flight vehicles which are under consideration for transportation systems. In addition to having direct and immediate practical application, these flows are sufficiently basic to invite intrinsic interest. When laminar and fully developed, they pose no great theoretical problems. If, however, they occur in the entrance region of a conduit, or if in the turbulent regime, the theoretical treatment of these flows may be only approximate. The stumbling block in the analysis is of mathematical nature in the first case; in the second case it originates mainly from a lack of satisfactory constitutive theory.

Types of Turbulence Models. In general, there are three main types of turbulence models, the first two of which employ Boussinesq's suggestion that the stress-rate of strain law for time-averaged turbulent flows could be represented in the same form as that for a Newtonian fluid in laminar motion. The first type are those models in which the turbulent viscosity is found by way of algebraic formulas, involving only properties of the mean velocity profile as unknowns; the second type are those models in which the

[1] Presently, Energy Consultant, Phoenix, Ariz.

Contributed by the Applied Mechanics Division for presentation at the National Conference of Applied Mechanics, University of Utah, Salt Lake City, Utah, June 15–17, 1976, of THE AMERICAN SOCIETY OF MECHANICAL ENGINEERS.

Discussion on this paper should be addressed to the Editorial Department, ASME, United Engineering Center, 345 East 47th Street, New York, N. Y. 10017, and will be accepted until June 1, 1976. Readers who need more time to prepare a Discussion should request an extension of the deadline from the Editorial Department. Manuscript received by ASME Applied Mechanics Division, November, 1974; final revision, June, 1975. Paper No. 76-APM-16.

turbulent viscosity is determined from the solution of the differential equations for one or more properties of the turbulent motion. The third class of models includes those which dispense with the notion of the effective turbulent transport properties and, instead, provide differential transport equations for the turbulent fluxes themselves.

Model Requirements. A basis for comparison, particularly interesting to those who pay for computer time at commercial rates, is the number of differential equations employed; for, the greater the number of equations, the greater is the computing time. Models referred to as the algebraic turbulent viscosity type employ no differential equations; they are the simplest ones available. Prandtl's mixing-length model is a representative of this class.

In our selection of turbulence models for the problem under investigation, we can best convey what is required of a turbulence model by naming four attributes we should like it to possess. They are (*i*) simplicity, (*ii*) economy of computer time, (*iii*) width of applicability, and (*iv*) accuracy. The first two requirements restrict our choices to algebraic models. The width of applicability is one of the main objectives of this study. Here we want to investigate the possibility of using the simple eddy viscosity correlations of fully developed flow for the coupled pressure and shear flows in channel entrance. The fourth requirement guides us in our final choice as to which models best predict the flow characteristics.

Selection of Turbulence Models. The choice of which turbulence models to employ in the mathematical analysis is mainly determined by the model requirements just discussed. The basic and most important requirement is the simplicity of the model. Since algebraic formulations of eddy viscosity are the simplest, the selection is restricted to this type of model. The selection was further restricted to one-equation models of turbulence that are applicable over the whole width of the channel. More sophisticated models, such as a number of "law-of-the-wall" models, were not chosen due to difficulties that might be encountered in the numerical procedure when one tries to match the laminar sublayer to the core region. It is believed that such models would give good results, but since good agreement with experimental data was already obtained using the simple one-equation models, it was felt that no additional advantage would be obtained from using more elaborate models.

Recent Studies

The development of the velocity profile in the entrance region of a channel under the influence of pressure and shear forces was first investigated by Szeri, et al. [1].[2] This analysis was restricted only to laminar regime and the analytical technique was based upon a linearization of the equation of motion.

For the development of the velocity profile in the turbulent regime a recent investigation [2] has been completed. In this case, the analysis is based upon the application of the finite-cell technique to the transformed form of the equations of motion in terms of vorticity and stream function. The conclusions of this research which have already been reported [3] state that the most satisfactory constitutive theory is the eddy viscosity model proposed by Reichardt [4].

The foregoing sources do not concern themselves with the development of pressure in the entrance region of generalized channel flows. This paper is an extension of the same line of research and is concerned first with the application of the method developed by Hai [2] to the problem of predicting the pressure development in the entrance region of generalized turbulent channel flows, and second with the evaluation of these predictions through comparison with experimental data. Since it has already been shown that Reichardt's local eddy viscosity model gives the best predictions of flow development in this type of flow, the results of this research are based upon Reichardt's local model.

Other models that were employed in the original study include Prandtl's mixing-length model, Schlicting's fourth-order polynomial model, and van Driest's local model. The comparison of the results obtained by using these models and their agreements with experimental data can be found in reference [3].

It is believed that this work supplements the previous work reported on the subject of generalized channel flows, and lays the foundation for future research in this field.

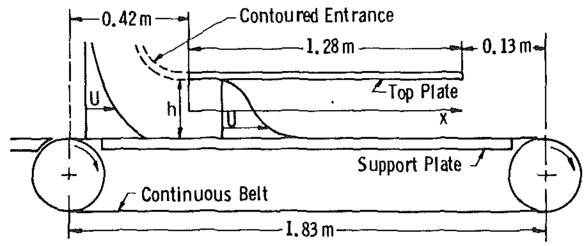

Fig. 1 Schematic representation of apparatus, dimensions approximate

Experimental Studies of Channel Flow

In order to investigate experimentally the coupling mechanism that exists between simple flows in the turbulent regime, a parallel plate-type apparatus is the best choice. Such apparatus was employed first by Reichardt [5] and shortly after by Robertson [6]. Each developed a belt-type apparatus to obtain plane-couette flows experimentally. Their apparatus, though conceptually similar, differed in design. Reichardt studied the flow phenomena using two moving surfaces, while Robertson's system consisted of a moving belt and a fixed plate. However, to achieve pure shear flow with only one boundary moving, he had to use an auxiliary fan to provide sufficient mass flow.

Recently, an apparatus with configuration similar to Robertson's was developed by Szeri, et al. [1]. The essential difference was the different entrance conditions; in Robertson's apparatus both the channel entrance and exit were over the pulley, while in the latter's apparatus the moving belt extended ahead of and behind the channel. Gada [7] and later Jaramillo [8] investigated the flow characteristics of generalized turbulent channel entrance region using the latter apparatus.

The work by Szeri, et al. [3], discusses the experimental results of Gada and Jaramillo and gives a full description of the experimental apparatus, so this will not be repeated here, except that Fig. 1 represents the experimental apparatus schematically.

In this work the experimental results of Gada [7] and Jaramillo [8] are used as bases for comparison with the predicted values of pressure development in the entrance region of generalized turbulent channel flows. For the case of fully developed turbulent channel flow, the experimental results of Laufer [9] are used for comparison with predicted results.

A word of caution is necessary at this point regarding the values of Reynolds number cited in this paper. Gada [7] claims that his measurements were taken at a Reynolds number of 8300, where the belt speed and channel height were taken as characteristic velocity and length, respectively. Unfortunately, this is not correct. Using the stated belt speed and channel height, one arrives at a Reynolds number of 6760. It seemed that a wrong value of kinematic viscosity had been used in the calculation. This assertion was later confirmed [2] and the values of Reynolds number have been corrected accordingly. Also, Laufer [9] gives the results of his experimental investigations for Reynolds numbers of 30,800 and 61,600. In his definition of the Reynolds number he uses the maximum velocity at the channel center line as the velocity parameter, and half height of the channel as the characteristic length parameter. Here, we have consistently based the Reynolds number on the full height of the channel, and hence Laufer's results for Reynolds numbers of 30,800 and 61,600 are comparable with our results for Reynolds numbers of 61,600 and 123,200, respectively.

Analysis

Governing Differential Equations. The fundamental conser-

[2] Numbers in brackets designate References at end of paper.

vation laws of mass and momentum provide the basic differential equations. Auxiliary relations for the transport properties and constitutive behavior supplement the differential equations; and the proper specification of the boundary condition equations make the mathematical problem complete.

In Cartesian tensor notation the differential equations of mass and momentum conservation take the following forms:

$$\rho_{,t} = -(\rho u_i)_{,i} \tag{1}$$

$$\rho(u_i)_{,t} = -(\rho u_i u_j + p\delta_{ij} - \tau_{ij})_{,j} + \rho B_i \tag{2}$$

The dependent variables have their usual fluid dynamic interpretation, with ρ the mass density, u_i the local velocity vector, B_i the applicable body force, τ_{ij} the stress tensor, and p the pressure. In these equations, the comma denotes vector differentiation of a tensor, while a comma by t indicates the partial derivative with respect to time.

The solution of these two equations requires specification of a constitutive relationship between the dependent variables, the stress tensor τ_{ij} and the viscosity μ. At this juncture, we assume that either (1) the fluid is Newtonian or (2) turbulent flow is adequately characterized by the laminar flow equations with the molecular viscosity replaced by a scalar effective viscosity. In both cases, the following equation defines the stress tensor constitutive relationship to velocity gradient and viscosity

$$\tau_{ij} = 2\mu(E_{ij} - \frac{1}{3}E_{kk}\delta_{ij}) \tag{3}$$

where

$$E_{ij} \equiv \frac{1}{2}(u_{i,j} + u_{j,i}). \tag{4}$$

It might be argued that this is a rather simplistic misrepresentation of the time-averaging and Reynolds stress modeling that comprise the development of analytical models for turbulent flow, because the effective viscosity model for turbulent shear is developed for shear stresses and the use of the same viscosity for normal stresses cannot be justified in a shear flow where the turbulence is anisotropic. Although this is a valid objection to the adoption of the aforementioned second assumption regarding the constitutive behavior of turbulent flow, yet many investigators such as Gosman, et al. [10], Baker [11], and Roache [12] recommend the use of this rather simplistic formulation in view of the fact that more sophisticated modeling is not warranted when one is only concerned with the macroscopic behavior of flow, or when the microscopic structure of turbulence is not of prime interest to the investigator. Moreover, the final judge is always the experimental data, and since good agreement between theory and experiment has been obtained for a variety of flow regimes using this simple modeling, the results of the theoretical analysis are satisfactory for most, if not all, engineering applications of this type of flow.

The value of the effective viscosity μ is obtained from Reichardt's local eddy viscosity model by the following relationships:

$$\mu = \mu_0 + \mu_t \tag{5}$$

$$\frac{\mu_t}{\mu_0} = 0.4[y^+ - 10.7 \tanh(y^+/10.7)] \tag{6}$$

where μ_0 is the molecular viscosity, μ_t is the turbulent or eddy viscosity, and y^+ is defined by

$$y^+ = y\frac{\rho u_1{}^+}{\mu_0}. \tag{7}$$

The local shear velocity, $u_1{}^+$, is given by

$$u_1{}^+ = \sqrt{\mu\left|\frac{\partial u_1}{\partial y}\right| \Big/ \rho}. \tag{8}$$

Development of Differential Equations of Motion. There are various points of view as to which of the possible forms of the equation of motion is most suitable for numerical solutions. Some workers, for example, Harlow and Welch [13] prefer to retain the velocities and pressure as dependent variables. However, the majority of researchers, such as Fromm [14], Aziz and Hellums [15], and Patankar and Spalding [16] feel that the coupling and nonlinearities associated with the presence of pressure in the equations make it advantageous to use the vorticity and stream function as dependent variables.

The derivation of the equations of motion in terms of vorticity and stream function is quite tedious when kept general. The reader will find these in detail in reference [2]. Here, only some results are cited.

The vorticity and the stream function are defined by the equations

$$\omega = \frac{1}{r^\alpha}\epsilon_{3ij}u_{j,i} \tag{9}$$

$$\rho u_i = \frac{1}{r\sin^\alpha\phi}\epsilon_{3ij}\psi_{,j} + \rho u_3\delta_{i3}. \tag{10}$$

Here, ω is the vorticity, ψ is the stream function, ϵ_{ijk} is the Cartesian alternating tensor, while α and r are defined as follows:

In equations (9) and (10), α is nonzero only for spherical coordinates when it is unity, r is set equal to unity (and $u_3 \equiv 0$) for rectangular coordinates. Equation (10) identically satisfies the continuity equation (1) in Cartesian, cylindrical, and spherical coordinate systems, for both compressible and unsteady incompressible flows. Further development of the equations of motion yield the following equations in terms of vorticity and stream function:

$$\omega = -\frac{1}{r^\alpha}\left(\frac{1}{\rho r\sin^\alpha\phi}\psi_{,k}\right)_{,k} \tag{11}$$

$$(\rho r^\alpha\omega)_{,t} = -\epsilon_{3ki}\left\{\left(\frac{r^\alpha\omega\psi_{,i}}{r\sin^\alpha\phi}\right)_{,k} + \frac{1}{2}\rho_{,k}\left(\frac{\psi_{,l}}{\rho r\sin^\alpha\phi}\right)^2_{,i} + \left[\rho u_3\epsilon_{3il}\left(\frac{\psi_{,l}}{\rho r\sin^\alpha\phi}\right)_{,3}\right]_{,k}\right\} + \left[\mu(r^\alpha\omega)_{,k} - \mu_{,k}(r^\alpha\omega) - 2\mu_{,j}\left(\frac{\psi_{,j}}{\rho r\sin^\alpha\phi}\right)_{,k}\right]_{,k} + \mu_{,k}\epsilon_{3ki}u_{3,3i}. \tag{12}$$

$$(\rho u_3)_{,t} = -\epsilon_{3ij}\left(\frac{\psi_{,j}}{r\sin^\alpha\phi}u_3\right)_{,i} - (\rho u_3 u_3)_{,3} - p_{,3} + (\mu\, u_{3,k})_{,k} + \frac{1}{3}\mu u_{3,33} + \mu_{,k}u_{k,3}. \tag{13}$$

The transformed form of the equations of motion in terms of vorticity and stream function are solved by a "successively converged" successive substitution finite-cell technique developed by Hai [2] and Gosman, et al. [10]. The details of the successive substitution technique are found in references [3, 10], and the method of "successive convergence" is discussed in reference [2]. These will not be repeated here, except to say a few words about the method of successive convergence.

Instead of recalculating the effective viscosity field at each stage of the method of successive substitutions, it was decided to work out intermediate convergent solutions with frozen effective viscosity profiles. Such an intermediate convergent solution was then used to evaluate the effective viscosity profile that was kept frozen during the next round of iterations by successive substitutions.

Boundary Conditions

Elliptic partial differential equations must be supported by conditions on the variables at all points of a closed boundary surrounding the field. Satisfactory boundary conditions for a dependent variable (ψ or ω) are of three general types:

1 The specifications of the values which ψ or ω must assume along the boundary.

2 The specification of the values of the component of the gradient of ψ or ω at the normal to the boundary.

3 The provision of some algebraic relation which connects the

value of ψ or ω to the values of their normal components along the boundary.

In fact, it is usual for values to be specified at some parts of a boundary, and for gradients to be specified at other parts. Also, when several differential equations are to be solved simultaneously, there is no need for the boundary conditions for each equation to be of the same type.

It is necessary here only to give examples of the boundary conditions which are encountered in our present problem. The field of flow is bounded in four ways:

1 By the stationary wall.
2 By the moving wall.
3 By the inlet end.
4 By the outlet end.

Each of these will be discussed separately. For simplicity the equations will be expressed in rectangular coordinates (x, y) for the case of steady incompressible flow applicable to the entrance flow problem.

Boundary Conditions at the Stationary Wall. *Stream Function.* Since the wall is impermeable to matter, the stream function must have a constant value along its whole length. The specification of this value, in the data of the problem, constitutes the boundary condition on the stream function for this part of the boundary.

Vorticity. It is rare for the vorticity at the wall to be specified, and even the vorticity gradient along the normal, which is connected with the pressure gradient along the wall, is not often known at the start. The boundary condition for the vorticity, therefore, has to be deduced from other information. Usually this is the requirement that there should be no slipping between the wall and the fluid adjacent to it.

Near a wall, gradients in the direction parallel to the wall are much smaller than those in the normal direction. They may, therefore, be neglected. Considering n to be the direction normal to the wall, the simplified form of equation (12) for the case of steady incompressible flow in rectangular coordinates can be integrated twice, to yield

$$\omega = \frac{A \int_0^n \exp\,[g(\eta)]d\eta + B}{\mu \exp\,[g(n)]} \tag{14}$$

with $g(\eta)$ defined as

$$g(\eta) = \int_0^\eta \frac{(\partial\psi/\partial x)}{\mu} d\zeta \tag{15}$$

where A and B are integration constants, and ζ and η are dummy variables.

We also need a second equation to link vorticity and stream function; this is equation (11), which yields the following after a double integration:

$$\psi - \psi_0 = -\int_0^n \rho \left[\int_0^\eta \omega d\zeta\right] d\eta. \tag{16}$$

Here, the no-slip condition has been introduced, for $(\partial\psi/\partial n)_0$ has been taken as zero. The subscript 0 refers to the value at the wall.

How equations (14) and (16) together yield the boundary condition for vorticity is best depicted by considering the case of uniform viscosity and zero mass transfer through the wall. Then the solution to these two equations becomes

$$\psi - \psi_0 = -\frac{\rho}{\mu}\left(\frac{An^3}{6} + \frac{Bn^2}{2}\right). \tag{17}$$

Now, B is equal to the vorticity at the wall, ω_0, multiplied by viscosity; and A is equal to the gradient of vorticity at the wall, $(\partial\omega/\partial n)_0$, multiplied by the same quantity. Thus equation (17) binds together the vorticity gradient and vorticity, and so constitutes a satisfactory boundary condition.

Boundary Conditions at the Moving Wall. *Stream Function.* As in the case of the stationary wall, since the wall is impermeable to matter, the boundary condition specification is the same.

Vorticity. If the wall moves at a velocity V_p in its own plane, we follow the same procedure as in the case of the stationary wall, with the exception of the no-slip condition. Instead of $(\partial\psi/\partial n)_0 = 0$, we have

$$\left(\frac{\partial\psi}{\partial n}\right)_0 = \rho V_p. \tag{18}$$

Upon using this boundary condition in the integration of equation (11), we obtain the following, instead of equation (16):

$$\psi - \psi_0 = -\int_0^n \rho \left[\int_0^\eta \omega d\zeta - V_p\right] d\eta. \tag{19}$$

Boundary Conditions at the Inlet End. *Stream Function.* The initial velocity profile $u_1(0, y)$ is known from the experimental data. Equation (10) is used to find the initial stream function profile.

$$\psi(0, y) = \rho \int_a^y u_1(0, \eta) d\eta \tag{20}$$

where $y = a$ is the point at which the stream function is considered to be zero.

Vorticity. The boundary condition on vorticity is the profile of vorticity distribution at the inlet boundary. Knowing the initial velocity distribution, Equation (9) is used to determine this profile.

$$\omega(0, y) = -\frac{\partial u_1(0,y)}{\partial y} \tag{21}$$

where the gradient of the y-component of velocity with respect to the x-direction has not been considered due to its negligible contribution to the vorticity profile.

Boundary Conditions at the Outlet End. Since the flow is considered to be fully developed at the outlet end, the gradients of stream function and vorticity with respect to the flow direction should vanish at the boundary. These provide the normal boundary conditions at the outlet end.

Recovery of Pressure

The purpose of introducing the vorticity and stream function was to allow pressure, p, to be eliminated from the equations, for its presence made them harder to solve. However, once the solution has been obtained, the pressure distribution is recovered from the vorticity-stream function characterization of this problem class by enforcing linear momentum conservation. Equation (2) can be transformed to the Laplacian on pressure by an additional differentiation and solved as a boundary-value problem. Since this is not a well-posed description for pressure, the preferable approach is to integrate the momentum equation [11].

Contract the momentum equation, in the absence of the body forces, with the infinitesimal vector, dx_i, and integrate, yielding

$$\int p_{,j}\delta_{ij}dx_i = -\int [\rho u_i u_j - \tau_{ij}]_{,j} dx_i - \frac{\partial}{\partial t}\int \rho u_i dx_i. \tag{22}$$

Note that the left-hand side of equation (22) is the integral of a perfect differential and thus independent of path. Hence the pressure at any point in the field can be determined, in comparison to some reference value, by integrating over an arbitrary (the easiest, of course) path between the two points. In the case of the problem under investigation, the formulation of the problem is simpler, since we are only concerned with two-dimensional flows. In such a case we have the following algorithm for the evaluation of pressure.

Knowing the velocity field, one is able to apply the principle of momentum conservation, and obtain the following two equations for the distribution of pressure in the two coordinate directions.

$$\frac{\partial p}{\partial x} = \frac{\partial}{\partial x}\left[\mu\left(2\frac{\partial u_1}{\partial x}\right) - \rho u_1{}^2\right] + \frac{\partial}{\partial y}\left[\mu\left(\frac{\partial u_1}{\partial y} + \frac{\partial u_2}{\partial x}\right) - \rho u_1 u_2\right] \tag{23}$$

$$\frac{\partial p}{\partial y} = \frac{\partial}{\partial x}\left[\mu\left(\frac{\partial u_1}{\partial y} + \frac{\partial u_2}{\partial x}\right) - \rho u_1 u_2\right] + \frac{\partial}{\partial y}\left[\mu\left(2\frac{\partial u_2}{\partial y}\right) - \rho u_2{}^2\right]. \quad (24)$$

Since the right-hand side of these two equations are known, a simple integration will yield the pressure difference between any two points in the flow field. In the special case of the flow in a channel, the variation of pressure in the y-direction is negligible in comparison to the variation of pressure in the x-direction. These equations have been used to evaluate the development of pressure in the entrance region of the channel.

When only the fully developed portion of the channel is considered, these equations take simpler forms. Here the partial derivatives with respect to x vanish, also we may assume that the second component of velocity (u_2) is negligible, and the pressure across the channel is uniform, i.e., $p = p(x)$. With these assumptions, equations (23) and (24) reduce to

$$\frac{dp}{dx} = \frac{\partial}{\partial y}\left[\mu\left(\frac{\partial u_1}{\partial y}\right)\right] \quad (25)$$

and

$$0 = \frac{\partial}{\partial}\left[\mu\left(\frac{\partial u_1}{\partial y}\right)\right]. \quad (26)$$

The simultaneous solution of these equations yields

$$\mu\frac{\partial u_1}{\partial y} = ky + \text{constant} \quad (27)$$

where k is the pressure drop per unit length in the x-direction such that

$$\frac{dp}{dx} = k. \quad (28)$$

If the interest is primarily on the fully developed region, then equation (27) can be used to evaluate k and hence determine the pressure drop.

Results and Discussion

Employing the foregoing algorithm and embodying it in the same computer program that calculates the velocity development in the channel entrance, we are able to predict the pressure variations for any Reynolds number and any inlet velocity profile.

Fig. 2 shows the experimental values of pressure development along the channel length for various Reynolds numbers. It is clear that the values of pressure drops (i.e., $p - p_{atm}$) are a function of Reynolds number and the distance from the channel entrance. Here Reynolds number is defined by

$$\text{Rey} = \frac{\rho_0 V_p h}{\mu_0} \quad (29)$$

where ρ is the fluid (in this case air) density, V_p is the belt velocity, h is the channel height, and μ_0 is the molecular viscosity.

All of the measurements reported in this paper were taken with a "round entrance" in position (see Fig. 1). The contour of this entrance consisted of a partial arc of 5.7 cm rad and its horizontal tangent plane 5.0 cm in length. The mass flow rate did not meet the requirement of pure shear (Couette) flow in any of the experiments. One parameter which affects this mass flow rate is the ratio of the length of the open belt upstream of the channel to the height of the channel. Average velocities of different experiments were calculated by numerically integrating the curve of the entrance velocity profiles. In the four cases where such profiles were available, the author discovered that all the average velocities were in the range of 38 to 41 percent of the belt velocity, showing an increase of 0.08 V_p to 0.11 V_p over the value reported by Robertson [6]. It is believed that this increase in mass flow rate was caused mainly by the presence of the open belt ahead of the channel. Robertson's apparatus did not have an open belt ahead of the channel entrance. It is a matter of conjecture at this point that by selecting the correct combination of entrance shape, channel aspect ratio, channel length, and length of the open belt ahead of the channel

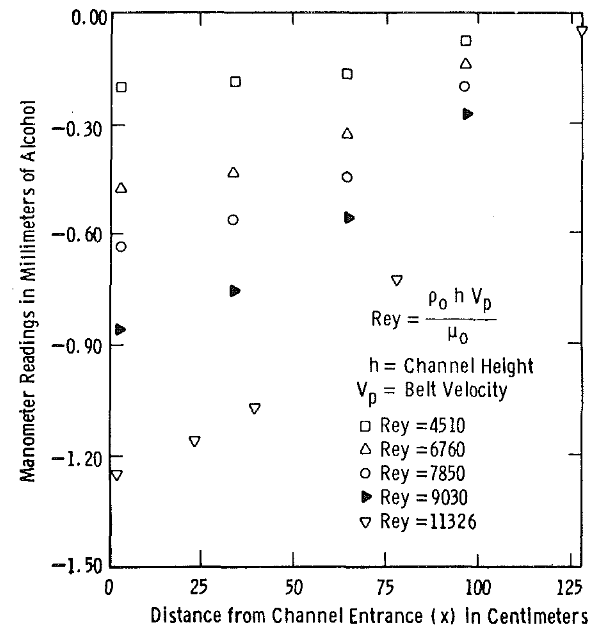

Fig. 2 Experimental values of pressure development in generalized channel entrance flow.

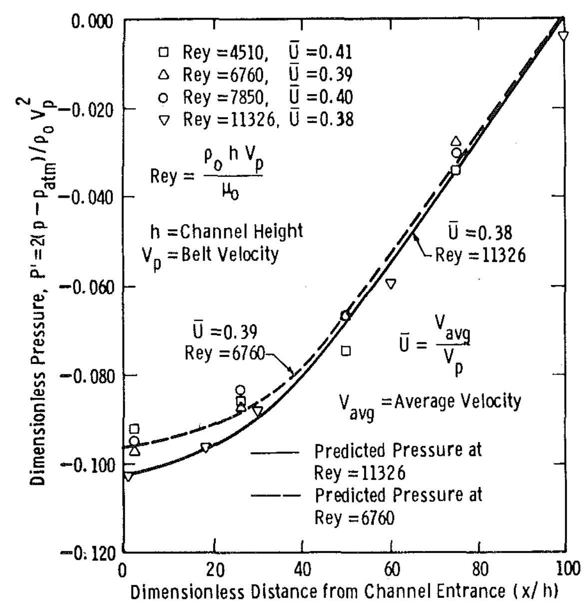

Fig. 3 Comparison of measured and predicted values of pressure development for various Reynolds numbers in generalized turbulent channel entrance flow

entrance, it would be feasible for a pure shear (Couette) flow to occur in a belt-type apparatus. In the experiments reported here, the data were all taken with the aforementioned variables being kept constant and only varying the Reynolds number via varying the belt speed. It is then believed that the minor variations among the values of average to belt speed ratios are due to experimental error, rather than due to another factor.

Since the data from the belt-type apparatus involves a pressure gradient, it is evidently a combined pressure (Poiseuille) and shear (Couette) flow, because shear flow alone will not have a pressure gradient. The pressure gradient is characterized by two parameters; one is the Reynolds number (Rey) and the other is ratio of average to belt velocity ($\bar{U} = V_{avg}/V_p$) which would be 0.5 for pure shear flows (with no pressure gradient).

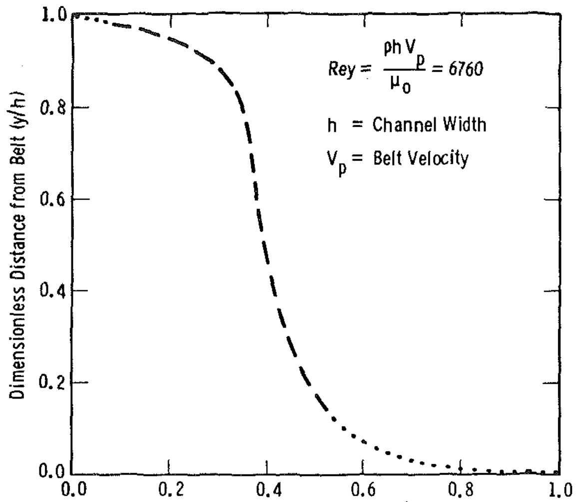

Fig. 4 Gada's experimentally determined turbulent velocity profile at the entrance to the channel

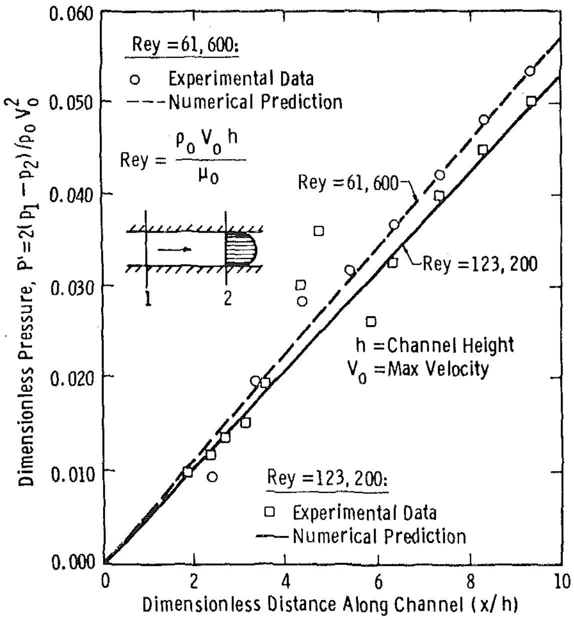

Fig. 5 Comparison of predicted pressure drop and Laufer's experimental data for fully developed turbulent channel flow

Little benefit is accrued from a representation such as Fig. 2, but if we plot the dimensionless pressure drop, $P' = 2(p - p_{atm})/\rho_0 V_p{}^2$, versus the dimensionless distance from the channel entrance (see Fig. 3), it becomes evident that the dimensionless pressure drop is not a very strong function of the Reynolds number. In this figure it is seen that the data coalesce to a very narrow band, and it cannot be ascertained what the effect of the second parameter (i.e., the ratio of average to belt velocity) is on the pressure drop, because all the data reported on Fig. 3 have values of $\bar{U} = V_{avg}/V_p$ within five percent of one another.

In fact, the values of $\bar{U}$ could be considered almost equal for all the cases shown, because the minor variations could be attributed to the experimental errors in the data and to the numerical errors in the integration procedure in obtaining the average velocity. With this in mind, the conclusions become more specific, in that the effect of the parameter $\bar{U}$ is eliminated from the analysis and the pressure drop profile exhibits only a weak dependence on Reynolds number.

Two distinct regions are seen in Fig. 3. The first region, which is effectively the entrance length of the channel and in which the flow development takes place, extends only to a distance of approximately 40 h. In this region the effect of the Reynolds number is more than the effect of the distance from the channel entrance. However, in the second region, which is essentially the fully developed region, the familiar straight-line pressure-drop curve is obtained with little dependence on Reynolds number.

The numerical prediction of the pressure drop for generalized channel entrance flow for Reynolds numbers of 6760 and 11,326 have been obtained and are displayed in Fig. 3. The comparison shows excellent agreement between experimental data and predicted values.

Schlichting [17] has shown that the entrance length (i.e., the dimensionless distance, x/h, from the channel entrance to the point of fully developed flow) is only a linear function of the Reynolds number for parallel plate channels and pipes. This is true only if we keep the shape of the inlet velocity profile the same. Schlichting has derived his results using a uniform velocity (i.e., a rectangular velocity) profile at the entrance to the channel or the pipe. It is evident that the entrance length is reduced as the shape of the entrance velocity profile approaches that of the fully developed profile, and this entrance length is reduced to zero when the entrance velocity profile is identical with the fully developed profile at which point the flow is fully developed at the entrance to the channel.

In view of the foregoing, one might conclude that

$$\frac{x}{h} = (\text{constant}) \cdot \text{Rey} \cdot \Phi$$

where Φ is a shape factor function which depends upon the degree to which the inlet velocity profile differs from the fully developed velocity profile.

In the experiments reported here, the inlet velocity distributions all had an S-shaped profile similar to the one shown on Fig. 1, but they differed to some extent from one another. A sample velocity profile at the channel entrance is shown in Fig. 4. All that could be said at this point is that the development length for these cases considered had x/h values of between 35 and 45 (or approximately 40). The reader is warned against using this criterion to situations other than those that closely resemble the velocity profile shape and Reynolds number range discussed in this paper. "Similar" velocity profiles, i.e., inlet velocity distributions whose nondimensionalized velocity profiles are identical to one another, have the same shape factor function Φ, and hence their x/h ratio can be represented by

$$\frac{x}{h} = (\text{constant}) \text{ Rey}.$$

Such similar velocity profiles have the same ratio of average to belt velocity ($\bar{U} = V_{avg}/V_p$). However, nonsimilar velocity profiles that have different shape factor functions (Φ) may have equal ratios of average to belt velocity. As an example, one may consider a set of two such profiles:

1 A uniform profile with $u_1(0, y) = 0.5\ V_p$.

2 A linearly varying profile with $u_1(0, y) = (1 - (y/h))V_p$. These two profiles have different shape factor functions, but they both have $\bar{U} = ½$.

An interesting case is to compare the experimental data and numerically predicted values of pressure drop in the fully developed portion of a simple channel flow for very high Reynolds numbers (of the order of 100,000). Such data exists in literature and is due to Laufer [9]. This case has already been solved by other mathematical techniques using various turbulence models and good agreement has been obtained with experimental data. The purpose of the numerical prediction here is not to present a duplication of past techniques, but rather to show that the present numerical technique and the adopted constitutive theory of turbulent flow can be used to predict the pressure development in such flows with accuracy and relative ease. Fig. 5 shows such a comparison where the present method of pressure recovery calculations for fully developed flow has been employed to predict the pressure drop in a channel for Reynolds numbers of 61,600 and 123,200. In this case also, the agreement is excellent and we obtain the straight-line relationship between the dimensionless pressure drop, $P' = 2(p_1 - p_2)/\rho_0 V_0^2$, and the dimensionless distance along the channel. There is little dependence of pressure drop on Reynolds number.

Conclusions

In closing, the following main conclusions are offered:

1 The vorticity-stream function formulation of the two-dimensional boundary-value problem in fluid mechanics which has been used to calculate the velocity development in the entrance region of generalized turbulent channel flows is also capable of yielding stable solutions for the pressure development in the entrance region, as well as fully developed region of channel flows.

2 If the actual values of manometer readings (pressure drops) are plotted versus the distance from the channel entrance, the data is very scattered; but when the dimensionless pressure drops are plotted versus the dimensionless distance from the channel entrance, the data coalesce to a very narrow band and two regions of flow are distinguished.

3 The entrance length necessary for flow development is a function of channel height, Reynolds number and shape of the entrance velocity profile for the flow regimes considered here.

4 The entrance length necessary for pressure development is approximately 40 times the channel height for the range of Reynolds numbers and the particular entrance velocity profiles considered in this investigation. This criterion cannot be applied to other flow geometries.

5 There is excellent agreement between the experimental data and predicted results for a wide range of Reynolds numbers considered (from approximately 5000 to approximately 120,000).

Acknowledgments

The author is indebted to Prof. C. C. Yates, Chairman of the Mechanical Engineering Department of the University of Pittsburgh, for his help in setting up the experimental apparatus, and to Dr. A. Z. Szeri and staff of the Computer Center at the University of Pittsburgh for their assistance during the course of this research.

References

1 Szeri, A. Z., Yates, C. C., and Gada, M. J., "Shear-Type Entrance Flow Into Parallel Plate Channels," *Proceedings of the Fluid Dynamics Symposium,* McMaster University, Hamilton, Ontario, June 25–27, 1970, Paper No. 2, 24 pp.

2 Hai, S. M., "Generalized Turbulent Channel Flows," unpublished PhD Dissertation, School of Engineering, University of Pittsburgh, 1974.

3 Szeri, A. Z., Yates, C. C., and Hai, S. M., "Flow Development in a Parallel Plate Channel," ASME Paper No. 75-LubS-4, presented at the Joint Fluids Engineering and Lubrication Conference, Minneapolis, Minnesota, May 5–7, 1975.

4 Reichardt, H., "Complete Representation of Turbulent Velocity Distribution in Smooth Pipes," *Zeitschrift für Angewandte Mathematik und Mechanik,* Vol. 31, 1951, p. 208.

5 Reichardt, H., "Über die Geschwindingkeitsverteilung in einer Geradlinigen Turbulenten Couettstromung," *Zeitschrift für Angewandte Mathematik und Mechanik,* Sonderheft, Vol. 36, 1956, pp. 526–529.

6 Robertson, J. M., "On Turbulent Plane Couette Flow," *Proceedings of the Sixth Midwestern Conference on Fluid Mechanics,* University of Texas, Austin, Texas, 1959.

7 Gada, M. G., "Development of an Apparatus for Pure Shear Flow Investigations," unpublished MS Thesis, School of Engineering, University of Pittsburgh, 1970.

8 Jaramillo, R. E., "An Experimental Investigation of the Turbulent Plane Couette Flow," unpublished MS Thesis, School of Engineering, University of Pittsburgh, 1972.

9 Laufer, J., "Investigation of Turbulent Flow in a Two-Dimensional Channel," NACA R-1053, 1951.

10 Gosman, A. D., et al., *Heat and Mass Transfer in Recirculating Flows,* Academic Press, London, 1969.

11 Baker, A. J., "Numerical Solution to the Dynamics of Viscous Fluid Flow by a Finite-Element Algorithm: A First Step Toward Computational Continuum Mechanics," *Proceedings of the Pacific Symposium on Hydrodynamically Loaded Shells,* Honolulu, Hawaii, October 11–15, 1971, 36 pp.

12 Roache, P. J., *Computational Fluid Dynamics,* Hermosa Publishers, Albuquerque, N. M., 1972.

13 Harlow, F. H., and Welch, J. E., "Numerical Calculations of Time Dependent Viscous Incompressible Flow of Fluid With Free Surface," *The Physics of Fluids,* Vol. 8, No. 12, 1965, pp. 2182–2189.

14 Fromm, J. E., "Numerical Solution of the Nonlinear Equations for a Heated Fluid Layer," *The Physics of Fluids,* Vol. 8, No. 10, 1965, pp. 1757–1769.

15 Aziz, K., and Hellums, J. D., "Numerical Solution of the Three-Dimensional Equations of Motion-Convection in Fluids Heated From Below," *The Physics of Fluids,* Vol. 10, No. 2, 1967, pp. 314–324.

16 Patankar, S. V., and Spalding, D. B., "A Finite-Difference Procedure for Solving the Equations of the Two-Dimensional Boundary Layer," *International Journal of Heat and Mass Transfer,* Vol. 10, No. 10, 1967, pp. 1389–1412.

17 Schlichting, H., *Boundary-Layer Theory,* 6th ed., McGraw-Hill, New York, 1968, pp. 176–178.